

# CONFLUENCE OF SWALLOWTAIL SINGULARITIES OF THE HYPERBOLIC SCHWARZ MAP DEFINED BY THE HYPERGEOMETRIC DIFFERENTIAL EQUATION

MASAYUKI NORO, TAKESHI SASAKI, KOTARO YAMADA, AND MASAOKI YOSHIDA

ABSTRACT. The papers [Gálvez et al. 2000, Kokubu et al. 2003, Kokubu et al. 2005] gave a method of constructing flat surfaces in the three-dimensional hyperbolic space. Such surfaces have generically singularities, since any closed nonsingular flat surface is isometric to a horosphere or a hyperbolic cylinder. In the paper [Sasaki et al. 2006], we defined a map, called the hyperbolic Schwarz map, from the one-dimensional projective space to the three-dimensional hyperbolic space by use of solutions of the hypergeometric differential equation. Its image is a flat front and its generic singularities are cuspidal edges and swallowtail singularities. In this paper we study the curves consisting of cuspidal edges and creation/elimination of swallowtail singularities depending on the parameters of the hypergeometric equation.

## CONTENTS

1.	Introduction	1
2.	Singularities of the image surface	2
3.	Confluence of swallowtail singularities	9
	References	11

## 1. INTRODUCTION

We consider the *hypergeometric differential equation*

$$x(1-x)u'' + \{c - (a+b+1)x\}u' - abu = 0,$$

where  $(a, b, c)$  are complex parameters. By a change of the unknown  $u$  by multiplying a non-zero function, we deform the equation into the SL-form:

$$u'' - q(x)u = 0,$$

where

$$\begin{aligned} q &= -\frac{1}{4} \left( \frac{1-\mu_0^2}{x^2} + \frac{1-\mu_1^2}{(1-x)^2} + \frac{1+\mu_\infty^2-\mu_0^2-\mu_1^2}{x(1-x)} \right) \\ &= -\frac{1}{4} \frac{(1-\mu_\infty^2)x^2 + (\mu_\infty^2 + \mu_0^2 - \mu_1^2 - 1)x + 1 - \mu_0^2}{x^2(1-x)^2}, \end{aligned}$$

and

$$\mu_0 = 1 - c, \quad \mu_1 = c - a - b, \quad \mu_\infty = b - a.$$

---

*Date:* February 20, 2007.

*2000 Mathematics Subject Classification.* 33C05, 53C42.

*Key words and phrases.* hypergeometric differential equation, hyperbolic Schwarz map, flat front, swallowtail singularity.

For two linearly independent solutions  $u_0$  and  $u_1$  to this equation, we define the (multi-valued) *hyperbolic Schwarz map*

$$(HS) \quad HS : X = \mathbf{C} - \{0, 1\} \ni x \mapsto H(x) = U(x) {}^t\bar{U}(x) \in \mathbf{H}^3,$$

where

$$U = \begin{pmatrix} u_0 & u'_0 \\ u_1 & u'_1 \end{pmatrix};$$

The image lies in the three-dimensional hyperbolic space  $\mathbf{H}^3$  identified with the space of positive  $2 \times 2$ -hermitian matrices modulo diagonal ones.

We remark that the (multi-valued) *Schwarz map*

$$(S) \quad S : X \ni x \mapsto u_0(x) : u_1(x) \in \mathbf{P}^1,$$

and the (multi-valued) *derived Schwarz map*

$$(DS) \quad DS : X \ni x \mapsto u'_0(x) : u'_1(x) \in \mathbf{P}^1,$$

are regarded as the maps with images in the ideal boundary of  $\mathbf{H}^3$ , which is identified with the complex projective line. The maps  $S$  and  $DS$  are connected by a one-parameter family of flat fronts in  $\mathbf{H}^3$  and the map  $HS$  is one member of this family. We refer to [Gálvez et al. 2000, Kokubu et al. 2003, Sasaki et al. 2007] for these maps.

The image surface of  $X$  under  $HS$  is one of flat fronts studied in [Kokubu et al. 2003]. The points 0 and 1 are singularities of the differential equation and they may define *ends* generally. On the other hand, it is well-known that generic singularities of fronts are *cuspidal edges* and *swallowtails*. In [Sasaki et al. 2006], we drew pictures of surfaces either when the monodromy group of the equation is finite or when it is the elliptic modular group, especially paying attention to the curves of cuspidal edges and to the swallowtail singularities.

In this paper, we study the motion of such singularities depending on the parameters  $a$ ,  $b$  and  $c$ . Actually, we treat the case where the parameters take special values:  $a = 1/2$ ,  $b = 1/2$  and  $c = 1 - p$ , where  $p$  is a real parameter. The reason why we treat this case is that the hypergeometric differential equation admits a rich symmetry in this case so that computational arguments work fairly well. Moreover, when  $p = 0$ , we succeeded to draw nice pictures as in [Sasaki et al. 2006]. When  $p$  takes a general value, the number of points in the plane  $X$  where the map  $HS$  has swallowtail singularities is counted and when  $p$  takes some special values, we encounter confluences of swallowtail singularities. Referring to the general theory of such confluences given in [Arnold 1976, Langevin et al. 1995], we study the happenings in our case and show that the three among the five types of confluences in [Langevin et al. 1995] really happen and one more type of confluence appears. From a computational point of view, we relied on the primary-decomposition algorithm of related ideals to get the special values of  $p$  and on computing the Sturm sequence associated with polynomials in order to count the number of swallowtail singularities.

## 2. SINGULARITIES OF THE IMAGE SURFACE

Relative to the differential equation in an SL-form above, the conditions on the coefficient  $q$  so that the surface has cuspidal edges and swallowtails are given as follows; we refer to [Sasaki et al. 2006].

**Lemma 2.1.** (1) *A point  $p \in X$  is a singular point of the hyperbolic Schwarz map  $HS$  if and only if  $|q(p)| = 1$ ,*

(2) a singular point  $x \in X$  of HS is equivalent to the cuspidal edge if and only if

$$q'(x) \neq 0 \quad \text{and} \quad q^3(x)\bar{q}'(x) - q'(x) \neq 0,$$

(3) and a singular point  $x \in X$  of HS is equivalent to the swallowtail if and only if

$$q'(x) \neq 0, \quad q^3(x)\bar{q}'(x) - q'(x) = 0, \\ \text{and} \quad \Re \left\{ \frac{1}{q} \left( \left( \frac{q'(x)}{q(x)} \right)' - \frac{1}{2} \left( \frac{q'(x)}{q(x)} \right)^2 \right) \right\} \neq 0.$$

We apply the lemma to the hypergeometric equation. The set  $\{|q| = 1\}$  is given as the curve

$$C = \{x; P_1(x, \bar{x}) = 0\},$$

where

$$P_1(x, \bar{x}) = |Q|^2 - 16|x^2(1-x)^2|^2$$

and

$$Q(x) = (1 - \mu_\infty^2)x^2 + (\mu_\infty^2 + \mu_0^2 - \mu_1^2 - 1)x + 1 - \mu_0^2.$$

The topological type of the curve  $C$  heavily depends on the number of real roots of the equation  $P_1 = 0$ . We next define  $R$  by

$$q' = -\frac{Q'x(1-x) - 2Q(1-2x)}{4x^3(1-x)^3} = \frac{-R(x)}{4x^3(1-x)^3},$$

$S$  by

$$q^3(x)\bar{q}'(x) - q'(x) = \frac{S(x, \bar{x})}{4^4 x^6 (1-x)^6 \bar{x}^3 (1-\bar{x})^3},$$

and  $T$  by

$$\frac{1}{q} \left( \left( \frac{q'(x)}{q(x)} \right)' - \frac{1}{2} \left( \frac{q'(x)}{q(x)} \right)^2 \right) = \frac{T(x, \bar{x})}{Q(x)Q(\bar{x})}.$$

We thus have three polynomials in  $x, \bar{x}, a, b$  and  $c$ :

$$R(x) = x(1-x)Q' - 2(1-2x)Q,$$

$$S(x, \bar{x}) = Q^3(x)R(\bar{x}) + 64x^3(1-x)^3\bar{x}^3(1-\bar{x})^3R(x),$$

$$T(x, \bar{x}) = x(1-x)Q(\bar{x})(-16Q^2 - 8(1-2x)QQ' + 6x(1-x)Q'^2 - 4x(1-x)QQ'').$$

We set

$$P_2 = \Re(S), \quad P_3 = \Im(S), \quad R_1 = \Re(R), \quad R_2 = \Im(R) \quad \text{and} \quad R_3 = \Re(T).$$

Then the singularity is a cuspidal edge if and only if

$$P_1 = 0, \quad \{P_2 \neq 0 \text{ or } P_3 \neq 0\}, \quad \{R_1 \neq 0 \text{ or } R_2 \neq 0\}$$

and is a swallowtail if and only if

$$P_1 = 0, \quad P_2 = 0, \quad P_3 = 0, \quad \{R_1 \neq 0 \text{ or } R_2 \neq 0\}, \quad R_3 \neq 0.$$

**2.1. Shape of the curve  $C$ .** We restrict our attention to the case  $(a, b, c) = (1/2, 1/2, c)$ , and set  $x = (1/2 + s) + it$  and  $c = 1 - p$ . The polynomials  $P_i$  and  $R_i$  are polynomials of  $p, s$  and  $t$ . They are symmetric relative to the reflections:  $s \leftrightarrow -s, t \leftrightarrow -t$  and  $p \leftrightarrow -p$ . Hence, we pay attention only to the case  $p \geq 0$  in the following. Since  $x = 0, 1$  are singularities of the coefficient  $q$ , the points  $(s, t) = (\pm 1/2, 0)$  are out of consideration.

Since  $Q = 2c - c^2 - x + x^2$  and  $D = -4x^2(1-x)^2$ ,  $P_1$  is a polynomial of total degree eight given as follows:

$$P_1 = 1/2 + 5/2s^2 - 2p^2s^2 + 16t^2s^4 - 16t^4s^2 - 64t^2s^6 - 96t^4s^4 - 64t^6s^2 + 6t^2s^2 \\ + 2t^2p^2 - 3/2p^2 - 16t^6 - 16t^8 - 5t^4 - 5/2t^2 - 5s^4 + 16s^6 - 16s^8 + p^4$$

The curve  $C = \{(s, t); P_1(p, s, t) = 0\}$  for each  $p$  changes its shape as in Figures 3 and 4, where the value of constants  $p_i$  will be given in the next subsection.

**2.2. Swallowtail points.** We study the set  $Z := \{(p, s, t); P_1 = P_2 = P_3 = 0\}$ . It is done by use of the primary-decomposition-algorithm that finds a set of generators of every minimal associated prime of the ideal  $I := \langle P_1, P_2, P_3 \rangle$  in the ring  $\mathbf{Q}[p, s, t]$ . The result is the following.

**Lemma 2.2.** *The set  $Z$  is the union of the sets defined by the following ideals.*

1.  $I_1 := \langle p - 1, (2s - 1)^2 + 4t^2 \rangle$
2.  $I_2 := \langle p - 1, (2s + 1)^2 + 4t^2 \rangle$
3.  $I_3 := \langle p + 1, (2s - 1)^2 + 4t^2 \rangle$
4.  $I_4 := \langle p + 1, (2s + 1)^2 + 4t^2 \rangle$
5.  $I_5 := \langle t, 4s^4 - s^2 - p^2 + 1 \rangle$
6.  $I_6 := \langle s, 8t^4 + 6t^2 + 2p^2 - 1 \rangle$
7.  $I_7 := \langle H_0(p, t), H_1(p, s, t), H_2(p, s, t), H_3(p, s, t) \rangle$ .

The polynomials  $H_0(p, t)$ ,  $H_1(p, s, t)$ ,  $H_2(p, s, t)$ ,  $H_3(p, s, t)$  are given in the appendix.

Although the result was obtained by a “black box” algorithm, it can be verified if we are allowed to use the method of finding Groebner basis. Let  $G$  be a Groebner basis of an ideal  $J$  with respect to a term order. We denote the remainder of a polynomial  $f$  by  $G$  by  $\text{NF}_G(f)$ . Then  $f \in J$  if and only if  $\text{NF}_G(f) = 0$ ; in this way, we can verify an ideal inclusion.

Lemma 2.2 is shown as follows. We first see  $I \subset I_i$ , which implies  $V(I_i) \subset Z$ . The converse inclusion  $Z \subset \bigcup_{i=1}^7 V(I_i)$  follows from  $\bigcup_{i=1}^7 V(I_i) = V(I_1 I_2 \cdots I_7)$  and  $I_1 I_2 \cdots I_7 \subset \sqrt{I}$ . In fact,  $I_1 I_2 \cdots I_7$  is generated by  $P := \{g_1 g_2 \cdots g_7; g_i \in I_i (i = 1, \dots, 7)\}$  and we can verify  $g^2 \in I$  for each  $g \in P$  by using a Groebner basis of  $I$ .

Lemma 2.2 implies that the set  $Z$  consists of

$$\begin{aligned} Z_1 &:= \{(p, s, 0); 4s^4 - s^2 - p^2 + 1 = 0\}, \\ Z_2 &:= \{(p, 0, t); 8t^4 + 6t^2 + 2p^2 - 1 = 0\}, \\ Z_3 &:= \{(p, s, t); H_0(p, t) = H_1(p, s, t) = H_2(p, s, t) = H_3(p, s, t) = 0\}. \end{aligned}$$

Figure 1 draws the set  $Z_1$  projected to the space  $(s, p)$ . The explicit representation is

$$s^2 = \left(1 \pm \sqrt{16p^2 - 15}\right) / 8, \quad p = \pm \sqrt{4s^4 - s^2 + 1}.$$

The right figure enlarges the upper part of the left figure. As we see later in the next subsection, the circles in the right figure denote those points that are worse than swallowtail singularity: the  $p$ -coordinate of the top one is 1, that of middle ones is  $p_5$ , and that of the bottom ones is  $p_3$ , where

$$\begin{aligned} p_3 &:= \sqrt{15}/4 \sim 0.9682458365, \\ p_5 &\sim 0.9713175204. \end{aligned}$$

Thus, for any value of  $p \in (p_3, 1)$ ,  $p \neq p_5$ , we have four swallowtail points, and for any value  $p > 1$  two swallowtail points, both on the axis  $\{t = 0\}$ .

For the set  $Z_2$ , to have real points, it is necessary and sufficient that  $-p_1 \leq p \leq p_1$ , where

$$p_1 := 1/\sqrt{2} \sim 0.7071067810.$$

The explicit relation is

$$t^2 = \left(-3 + \sqrt{17 - 16p^2}\right) / 8, \quad p = \pm \sqrt{1/2 - 3t^2 - 4t^4}.$$

For each value  $p \in [0, p_1)$  we have two swallowtail points lying on the line  $\{s = 0\}$ . In the case  $p = p_1$ , the point  $(s, t) = (0, 0)$  is not a swallowtail.

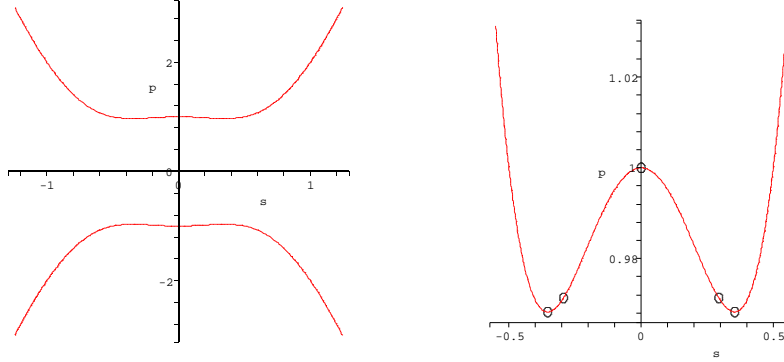


FIGURE 1. The set  $Z_1$  projected to the space  $(s, p)$

Summarizing the argument above, the number of the swallowtail points belonging to  $Z_1 \cup Z_2$  is given as follows:

$p$	0	*	$p_1$	*	$p_3$	*	$p_5$	*	1	*
$Z_1$	0	0	0	0	0	4	2	4	0	2
$Z_2$	2	2	0	0	0	0	0	0	0	0

Here \* stands for any value between the values of the both sides.

To study the set  $Z_3$ , we first deal with the polynomials  $H_2$  and  $H_3$ . We can write

$$H_1(p, s, t) = c_1(p)s^2 + c_0(p, t),$$

where

$$c_1 = -8192000p^{18} + 71680000p^{16} - 267673600p^{14} + 565094400p^{12} - 749209600p^{10} + 651990400p^8 - 375410912p^6 + 138995680p^4 - 30234388p^2 + 2960012.$$

Then we can see that

- $c_1H_2$  and  $(c_1)^2H_3$  belong to the ideal  $\langle H_0, H_1 \rangle$ , which is verified by showing  $c_1H_2 \bmod H_0$  and  $(c_1)^2H_3 \bmod H_0$  are divisible by  $H_1$ .

Hence, for each value where  $c_1(p) \neq 0$ , the set  $Z_3$  is the same as the set  $\{H_0 = H_1 = 0\}$ . Moreover, we can see that

- $c_0^2$  belongs to the ideal  $\langle c_1, H_0 \rangle$  because  $c_1$  divides the remainder  $c_0^2 \bmod H_0$  with respect to  $t$ .

Hence, the set  $\{(p, s, t); p \geq 0, c_1 = H_0 = H_1 = 0\}$  consists of lines in  $(p, s, t)$ -space defined by  $c_1(p) = H_0(p, t) = 0$ , which are given as

$$(p, t) = (p_4, \pm 0.011811323560992964937), \\ (p_7, \pm 0.000192205787502698965), \\ (p_{10}, \pm 0.022606558445778182272),$$

where

$$p_4 \sim 0.97127920368420120746, \\ p_7 \sim 1.00370488167353310415, \\ p_{10} \sim 1.03276891081183183482.$$

The set  $\{(p, s, t); p \geq 0, c_1 = H_0 = H_1 = H_2 = H_3 = 0\}$  consists of the points

$$(p, s, t) = (p_4, \pm 0.4448235948, \pm 0.01181132356), \\ (p_4, \pm 0.2944179698, \pm 0.01181132356), \\ (p_7, \pm 0.5074847467, \pm 0.00019220578).$$

Taking care of these exceptions, it is enough to study the set  $\{(p, s, t); H_0 = H_1 = 0\}$ .

We next deal with the curve  $H_0(t, p) = 0$  in the  $tp$ -plane where  $p \geq 0$ ; look at Figure 2. In order to know the precise shape of the curve, we use the Sturm sequence. For a polynomial  $f(t)$ , the Sturm sequence  $\{f_0, f_1, \dots, f_l\}$  is defined by the following recurrence:

$$(2.1) \quad f_0 = f, f_1 = \frac{df}{dt}, f_i = -(f_{i-2} \bmod f_{i-1}) \quad (i = 2, \dots, l), f_{l-1} \bmod f_l = 0,$$

where  $(f_i \bmod f_{i-1})$  is the polynomial remainder. We define  $\sigma(a)$  to be the number of sign changes in the sequence  $\{f_0(a), f_1(a), \dots, f_l(a)\}$ , where zeros are not counted.

**Theorem 2.3.** (*Sturm*)[Jacobson 1975] *For  $a, b \in \mathbf{R}$  such that  $a < b$  and  $f(a), f(b) \neq 0$ , the number of roots of  $f(t)$  in the interval  $(a, b)$  is  $\sigma(a) - \sigma(b)$ . In particular, the number of all real roots of  $f(x)$  is determined by the signs of the leading coefficients and the degrees of  $f_i$ 's.*

Let  $\ell = \{f_0(t), \dots, f_l(t)\}$  ( $f_i \in \mathbf{Q}(p)[t]$ ) be a sequence of polynomials obtained by applying the recurrence (2.1) to  $f_0 = H_0$  with respect to  $t$ . Let  $M \subset \mathbf{R}$  be the zeros of the numerators and denominators of the leading coefficients of  $f_i$ 's.  $\mathbf{R} \setminus M$  is a disjoint union of open intervals  $I_k$ . Then the sequence  $\ell$  gives the correct Sturm sequence at each  $p \in \mathbf{R} \setminus M$  and Theorem 2.3 ensures that the number of roots of  $H_0$  is constant for all  $p \in I_k$ . It is clear that each branch  $t = t(p)$  such that  $H_0(p, t(p)) = 0$  over  $I_k$  is a continuous function of  $p$ . If  $p \in M$ ,  $p$  is a root of an irreducible polynomial over  $\mathbf{Q}$  and we can compute the Sturm sequence over an algebraic number field  $\mathbf{Q}(p)$ . The Sturm sequence at each  $p$  tells the number of roots  $t(p)$  within any interval, and we can draw the curve with desired precision.

The set  $M$  contains the zeros of the discriminant of the equation  $H_0 = 0$ , and we get the coordinates  $(p, t)$  of several extreme points as in the figure:

$$\begin{aligned} X &= (p_{10}, 0.02260655844), \quad A = (p_9, 0.02095131175), \\ B &= (p_8, 0), \quad C = (p_6, 0), \quad D = (p_5, 0), \\ E &= (p_4, 0.01181132356), \quad F = (p_2, 0.08654627008), \end{aligned}$$

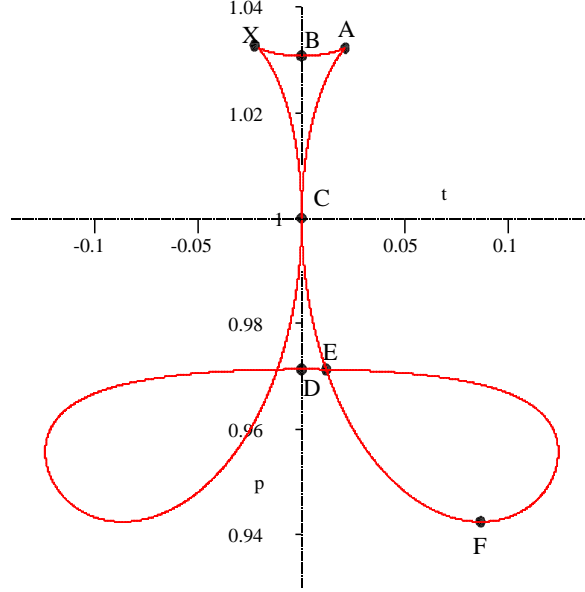
where

$$\begin{aligned} p_2 &\sim 0.94237741898935061, \\ p_6 &= 1, \\ p_8 &\sim 1.03077640441513745, \\ p_9 &\sim 1.03230371163023017. \end{aligned}$$

(Since the point  $X$  is very near to  $A$ , the point  $(p_{10}, -0.0226065584)$  is drawn in the figure.)

For each point  $(p, t)$  on the curve  $H_0(p, t) = 0$ , we solve the equation  $H_1(p, s, t) = 0$ . Then, since  $H_1(p, s, t) = c_1(p)s^2 + c_0(p, t)$ , the number of real solutions depends on the signs of  $c_1(p)$  and  $c_0(p, t)$ . To determine the sign of  $c_0(p, t)/c_1(p)$ , we enlarge the set  $M$  by adjoining the values of  $p$  satisfying  $c_0 = H_0 = 0$  for some  $t$ , and the zeros of  $c_1$ , and then recompute  $I_k$ . Let  $t = t(p)$  be the continuous function over  $I_k$  discussed above. Then  $c_0(p, t(p))/c_1(p)$  is also continuous and its sign is constant over  $I_k$  because the numerator does not vanish over  $I_k$ . Thus we can determine the the number of solutions by evaluating  $c_0(p, t(p))/c_1(p)$  at a point  $p \in I_k$ . For  $p \in M$ , we have to deal with an algebraic number field again; we omit the details.

**2.3. Non-swallowtail points.** If for some  $p$  the point  $(s, t)$  is a swallowtail, then  $(p, s, t) \in Z$ . However, not all points in  $Z$  are swallowtails. We need to check the condition  $(R_1 \neq 0$  or  $R_2 \neq 0)$  and the condition  $R_3 \neq 0$ , namely, the condition

FIGURE 2. The curve  $c_1(t, p) = 0$ 

$q' \neq 0$  and the condition  $\Re(T) \neq 0$ , respectively. This check is done by studying the sets

$$E_1 := \{(p, s, t); p \geq 0, P_1 = P_2 = P_3 = R_1 = R_2 = 0\}$$

and

$$E_2 := \{(p, s, t); p \geq 0, P_1 = P_2 = P_3 = R_3 = 0\},$$

by relying on the primary decomposition of the corresponding ideals  $\langle P_1, P_2, P_3, R_1, R_2 \rangle$  and  $\langle P_1, P_2, P_3, R_3 \rangle$ .

**Lemma 2.4.** *The set defined by the ideal  $\langle P_1, P_2, P_3, R_1, R_2 \rangle$  is the union of the sets defined by the ideals.*

- |                                   |   |
|-----------------------------------|---|
| 1. $[p - 1, t, s],$               | 2. $[p - 1, t, 2s - 1],$                  |
| 3. $[p - 1, t, 2s + 1],$          | 4. $[p - 1, 4s - 1, 16t^2 + 1],$          |
| 5. $[p - 1, 4s + 1, 16t^2 + 1],$  | 6. $[p - 1, s, 4t^2 + 1],$                |
| 7. $[p + 1, t, s],$               | 8. $[p + 1, t, 2s - 1],$                  |
| 9. $[p + 1, t, 2s + 1],$          | 10. $[p + 1, 4s - 1, 16t^2 + 1],$         |
| 11. $[p + 1, 4s + 1, 16t^2 + 1],$ | 12. $[p + 1, s, 4t^2 + 1],$               |
| 13. $[2p^2 - 1, t, s],$           | 14. $[16p^2 - 17, t, 8s^2 - 3],$          |
| 15. $[16p^2 - 15, t, 8s^2 - 1],$  | 16. $[16p^2 - 17, s, 8t^2 + 3],$          |
| 17. $[16p^2 - 15, s, 8t^2 + 1],$  | 18. $[20p^2 - 19, 80t^2 + 3, 80s^2 - 3].$ |

By this lemma we can see the following. The ideals 4, 5, 6, 10, 11, 12, 16, 17 and 18 have no real points. The ideals 1, 2, 3, 7, 8 and 9 yield three points

$$(1, 0, 0), \quad (1, \pm 1/2, 0),$$

and the ideals 13, 14 and 15 yield 5 points

$$(p_1, 0, 0), \quad (p_8, \pm s_1, 0), \quad (p_3, \pm s_2, 0),$$

in  $E_1$  (recall we assumed  $p \geq 0$ ), where

$$p_8 = \sqrt{17}/4 \sim 1.03077640, \quad s_1 = \sqrt{3/8} \sim 0.61237, \quad s_2 = 1/\sqrt{8} \sim 0.35355.$$

**Lemma 2.5.** *The set defined by the ideal  $\langle P_1, P_2, P_3, R_3 \rangle$  is the union of the sets defined by the ideals.*

$$\begin{array}{ll}
19. & [p-1, 4s^2-4s+4t^2+1], & 20. & [p-1, 4s^2+4s+4t^2+1], \\
21. & [p+1, 4s^2-4s+4t^2+1], & 22. & [p+1, 4s^2+4s+4t^2+1], \\
23. & [4p^2-3, 4s-1, 16t^2+1], & 24. & [4p^2-3, 4s+1, 16t^2+1], \\
25. & [r_1(p), s, r_2(p, t)], & 26. & [r_3(p), t, r_4(p, s)], \\
27. & [r_5(p), r_6(p, s), r_7(p, t)]. & & 
\end{array}$$

where

$$\begin{array}{ll}
r_1(p) & = 256p^6 - 464p^4 + 224p^2 - 19, \\
r_2(p, t) & = 24t^2 + 64p^4 - 84p^2 + 29, \\
r_3(p) & = 256p^6 - 560p^4 + 416p^2 - 109, \\
r_4(p, s) & = 24s^2 - 64p^4 + 108p^2 - 47, \\
r_5(p) & = 262144p^{14} - 1458176p^{12} + 3352128p^{10} - 4064896p^8 + 2723312p^6 \\
& \quad - 934456p^4 + 111981p^2 + 7964, \\
r_6(p, s) & = 105137152s^2 + 805737070592p^{12} - 3734052323328p^{10} + 6842337426624p^8 \\
& \quad - 6160590983296p^6 + 2674420712784p^4 - 400807788840p^2 - 27034171281, \\
r_7(p, t) & = 105137152t^2 + 1275266859008p^{12} - 6003856457728p^{10} + 11187800841024p^8 \\
& \quad - 10256897785728p^6 + 4544374234288p^4 - 701552747480p^2 - 45094112399.
\end{array}$$

In this lemma, the cases 19, 20, 21 and 22 yield two points

$$(1, \pm 1/2, 0)$$

in  $E_2$ , and the cases 23, 24 and 25 yield no real points. For the ideal 26, by solving  $r_3(p) = 0$ , we get a real positive solution  $p = p_5$ . The corresponding values of  $s$  are determined by the equation  $r_4(p, s) = 0$ . We thus have two points

$$(p_5, \pm 0.2939504177, 0)$$

in  $E_2$ . For the last ideal 27, by solving  $r_5(p) = 0$ , we get real positive solutions  $p = p_2$  and  $p_9$ . The corresponding values of  $(s, t)$  are determined by solving  $r_6(p, s) = r_7(p, t) = 0$ . The result is

$$(p_2, \pm 0.3834951026, \pm 0.08654627008), (p_9, \pm 0.5955418899, \pm 0.02095131175).$$

Summarizing the argument above, the number of the swallowtail points belonging to  $Z_3$  where  $p \geq 0$  is given as follows:

$p$	$p_2$	*	$p_5$	*	$p_6 = 1$	*	$p_8$	*	$p_9$	*
$Z_3$	0	8	4	4	0	4	4	8	0	0

**2.4. Number of swallowtail singularities.** As we mentioned earlier, we restrict our consideration to the range of  $p$  to the interval  $[0, \infty)$ . Combining the consideration in the previous two subsections, the exceptional values of  $p$  for which the point  $(p, s, t)$  in  $Z$  is not a swallowtail are

$$(2.2) \quad p_1, p_2, p_3, p_5, p_6 = 1, p_8, p_9.$$

We remark that the values  $p_4$  and  $p_7$  that appeared in the course of study of the set  $Z$  turn out to be not exceptional and that the exceptional values of  $p$  are classified into the three cases:

$$\begin{array}{l}
q' = 0 \text{ and } \Re(T) \neq 0 : p_1, p_3, p_6 \text{ at } (0, 0), p_8, \\
q' \neq 0 \text{ and } \Re(T) = 0 : p_2, p_5, p_9, \\
q' = 0 \text{ and } \Re(T) = 0 : p_6 \text{ at } (\pm 1/2, 0).
\end{array}$$

Now we sum up the above data and get the number  $N$  of swallowtail singularities:

$p$	0	*	$p_1$	*	$p_2$	*	$p_3$	*	$p_5$	*	$p_6 = 1$	*	$p_8$	*	$p_9$	*
$N$	2	2	0	0	0	8	8	12	6	8	0	6	6	10	2	2

In Figures 3 and 4, the swallowtail singularities are represented by circles; other symbols represent worse singularities explained in the next section.

*Remark 2.6.* The number  $N$  counts the swallowtail singularities in the plane  $x = 1/2 + s + it$ , *not* on the image surface; recall that the hyperbolic Schwarz map  $HS$  is multi-valued.

### 3. CONFLUENCE OF SWALLOWTAIL SINGULARITIES

In the previous section, we studied the variation of the number of swallowtail singularities when  $p$  runs from 0 to  $\infty$ . On the other hand, the confluence of swallowtail singularities was studied by Arnold [Arnold 1976]. Figure 6 cites the Figure 3 of [Langevin et al. 1995](p. 547), which shows five types  $(1, \dots, 5)$  of confluence (bifurcation) of swallowtail singularities.

From the study in the last section, we *observe* that the types 2, 3 and 5 actually occur in our move, and that another type of confluence also occurs. In Figures 3 and 4, they are denoted by

$$\bullet \text{ (Type 2), } \blacksquare \text{ (Type 3), } \blacklozenge \text{ (Type 5), } \odot,$$

respectively.

In this section, the (local) image surface is denoted by  $\mathcal{S}$ , and the (local) image of the curve  $\mathcal{C}$  under the hyperbolic Schwarz map  $HS$  is denoted by  $\mathcal{C}(\subset \mathcal{S})$ .

**3.1.  $\bullet$  Around  $p = p_1$ ,  $p = p_3$ ,  $p = p_6$  and  $p = p_8$ .** When  $p < p_1$ , there is a pair of swallowtail singularities on  $\mathcal{S}$  carried by a pair of cuspidal components of  $\mathcal{C}$ . When  $p$  tends to  $p_1$ , two singularities come together and kiss, and when  $p_1 < p$ ,  $\mathcal{C}$  becomes a pair of nonsingular curves. We observe that this move is of type 2 in Figure 6. See Figure 7 of the image surface  $\mathcal{S}$  under  $HS$  of the square  $\{(s, t); -0.5 < s < 0.5, -0.5 < t < 0.5\}$ . Similar happens when  $p \searrow p_3, p \searrow p_8$  and  $p \nearrow p_6$  around  $(s, t) = (0, 0)$ .

**3.2.  $\blacklozenge$  Around  $p = p_2$  and  $p = p_9$ .** When  $p \leq p_2$ , there are no swallowtail singularity. However, when  $p > p_2$ , there are four pairs of swallowtail singularities, eight in all. The move around  $p_2$  is observed to be of type 5 in Figure 6. A picture of a pair is drawn in Figure 8(left) when  $p = 0.945$ . The lower picture is the curve  $\mathcal{C}$  carrying two swallowtails, which reside at the two cusps of this curve. The upper picture is a tubular neighborhood in the surface  $\mathcal{S}$  of this curve  $\mathcal{C}$ . Similar happens when  $p \searrow p_9$ .

**3.3.  $\odot$  Around  $p = p_5$ .** When  $p \nearrow p_5$ , three swallowtail singularities shrink to one point that is not a swallowtail singularity and, instantly after passing  $p_5$  one swallowtail singularity reappears. This move is not in the five moves of Arnold in Figure 6. Figure 8(right) shows the curve  $\mathcal{C}$  with three cusps, and the surface  $\mathcal{S}$  around this curve.

**3.4.  $\blacksquare$  Around  $p = p_6$ .** When  $p = p_6 = 1$ , there are no swallowtail. If  $p$  goes apart from 1, then three swallowtail singularities appear in both directions; this move is observed to be of type 3 in Figure 6. In Figure 9, the left picture is the image of a small square situated right of the point  $(s, t) = (-0.5, 0)$  (singular point of the differential equation) including three swallowtails when  $p = 0.975$ . They shrink to one point as  $p$  tends to 1. The right picture is the image of a small square situated left of the point  $(-0.5, 0)$  including three swallowtails when  $p = 1.028$ .

**3.5. Drawing Figures.** We give some assignments on the figures. Figures 3–5 draw the curve  $\mathcal{C}$ . Each first row gives a global view and the second row for  $p \geq 0.78$  gives a finer view of a part of  $\mathcal{C}$ . The marks  $\bullet$ ,  $\blacksquare$ ,  $\blacklozenge$  and  $\odot$  are drawn in a somewhat emphasized manner. In the third row (in the second row when  $p \leq p_1$ ), the images curves  $\mathcal{C}$  are given; the range of drawing is indicated by a dotted quadrangle in the figures of the first rows. When  $p < 1$ , the map  $HS$  defined

in the upper half plane is continued analytically through the interval  $\{0 < x < 1\}$ , and, when  $p > 1$ , through the negative real axis  $\{x < 0\}$ . Figure 7 draws the images  $\mathcal{S}$  of the square  $\{(s, t); s \in (-0.5, 0.5), t \in (-0.5, 0.5)\}$ , where the image curves  $\mathcal{C}$  are drawn more in detail than in Figure 3. Figures 8 and Figure 9 draw  $\mathcal{S}$  and  $\mathcal{C}$  for distinct values of  $p$ .

### Appendix: List of polynomials

$$\begin{aligned}
H_0 = & (262144p^8 - 524288p^6 + 262144p^4)t^8 \\
& + (524288p^{10} - 1572864p^8 + 1687552p^6 - 735232p^4 + 79872p^2 + 16384)t^6 \\
& + (393216p^{12} - 1654784p^{10} + 2817024p^8 - 2459136p^6 + 1142464p^4 - 260480p^2 + 21700)t^4 \\
& + (131072p^{14} - 737280p^{12} + 1755392p^{10} - 2289728p^8 + 1761920p^6 - 794968p^4 + 192308p^2 - 18715)t^2 \\
& + 16384p^{16} - 118784p^{14} + 376000p^{12} - 679104p^{10} + 766068p^8 - 553296p^6 \\
& + 250232p^4 - 64912p^2 + 7412, \\
H_1 = & (-8192000p^{18} + 71680000p^{16} - 267673600p^{14} + 565094400p^{12} - 749209600p^{10} \\
& + 651990400p^8 - 375410912p^6 + 138995680p^4 - 30234388p^2 + 2960012)s^2 \\
& + (-83886080p^{16} + 461373440p^{14} - 1033895936p^{12} + 1196949504p^{10} \\
& - 740818944p^8 + 222822400p^6 - 22544384p^4)t^6 \\
& + (-125829120p^{18} + 786432000p^{16} - 2102657024p^{14} + 3123380224p^{12} - 2789900288p^{10} \\
& + 1502928896p^8 - 452747264p^6 + 55562240p^4 + 4239360p^2 - 1409024)t^4 \\
& + (-62914560p^{20} + 458424320p^{18} - 1490173952p^{16} + 2838306816p^{14} - 3490809856p^{12} \\
& + 2877347840p^{10} - 1598347904p^8 + 588634656p^6 - 138705184p^4 + 19590612p^2 - 1352780)t^2 \\
& - 10485760p^{22} + 94371840p^{20} - 391053312p^{18} + 980131840p^{16} - 1640966144p^{14} + 1914822656p^{12} \\
& - 1580043904p^{10} + 917850432p^8 - 366915360p^6 + 96240468p^4 - 15040195p^2 + 1087441. \\
H_2 = & (-172748519424t^2 + 342090457088000p^{16} - 2647506597888000p^{14} + 8502392953446400p^{12} \\
& - 15007782165760000p^{10} + 16125961477836800p^8 - 10936659362160000p^6 + 4626862256233568p^4 \\
& - 1127440491359040p^2 + 122038029361684)s^2 \\
& + (3503006280581120p^{14} - 15725697150484480p^{12} + 27286047559778304p^{10} - 22422671555297280p^8 \\
& + 8286510388346880p^6 - 927195522924544p^4)t^6 \\
& + (5254509420871680p^{16} - 27529427791380480p^{14} + 59988842462314496p^{12} - 6983053122779072p^{10} \\
& + 45967246621245440p^8 - 16318586888937472p^6 + 2406740047872000p^4 + 118811578937344p^2 \\
& - 58122468702208)t^4 \\
& + (2627254710435840p^{18} - 16487753934110720p^{16} + 45567759200370688p^{14} - 72489552047398912p^{12} \\
& + 72546907718641664p^{10} - 46869348690018304p^8 + 19388801939481216p^6 - 4981168098598560p^4 \\
& + 752756242889920p^2 - 55743159881812)t^2 \\
& + 437875785072640p^{20} - 3498277391564800p^{18} + 12794850594193408p^{16} - 2800194022336448p^{14} \\
& + 40236544719603712p^{12} - 39314960801359872p^{10} + 26264510377602688p^8 - 11791213573216192p^6 \\
& + 3403925190427360p^4 - 576100608409972p^2 + 44796791787623, \\
H_3 = & -43273504115712s^4 + (-174591366701056000p^{16} + 1354597407135744000p^{14} - 4361070217826508800p^{12} \\
& + 7714396815022745600p^{10} - 8303627443711283200p^8 + 5639582815676545920p^6 \\
& - 238886969950578656p^4 + 582795932673655872p^2 - 63153571220692772)s^2 \\
& + (-1787815595018813440p^{14} + 8060676765258874880p^{12} - 14035315945780543488p^{10} \\
& + 11564439040729546752p^8 - 4282247261844406272p^6 + 480262996655341568p^4)t^6 \\
& + (-2681723392528220160p^{16} + 14102307692284477440p^{14} - 30819600746391273472p^{12} \\
& + 35956859092128694272p^{10} - 23711874589423796224p^8 + 8431178804896194560p^6 \\
& - 1246058944783564800p^4 - 60931259457007616p^2 + 30059710795074560)t^4 \\
& + (-1340861696264110080p^{18} + 8440901125082644480p^{16} - 23384966557443178496p^{14} \\
& + 37273429941273878528p^{12} - 37362998720665520128p^{10} + 24170842385410605056p^8 \\
& - 10009973619071190144p^6 + 2574206274932313888p^4 - 389407674475545536p^2 \\
& + 28850050377704036)t^2 \\
& - 223476949377351680p^{20} + 1789753918478090240p^{18} - 6558969382275055616p^{16} \\
& + 14379092033155440640p^{14} - 20693107121308362752p^{12} + 20246624022842148864p^{10} \\
& - 13542078892737183872p^8 + 6086106587227785920p^6 - 1758722499457332320p^4 \\
& + 297968123692665860p^2 - 23197985921481043.
\end{aligned}$$

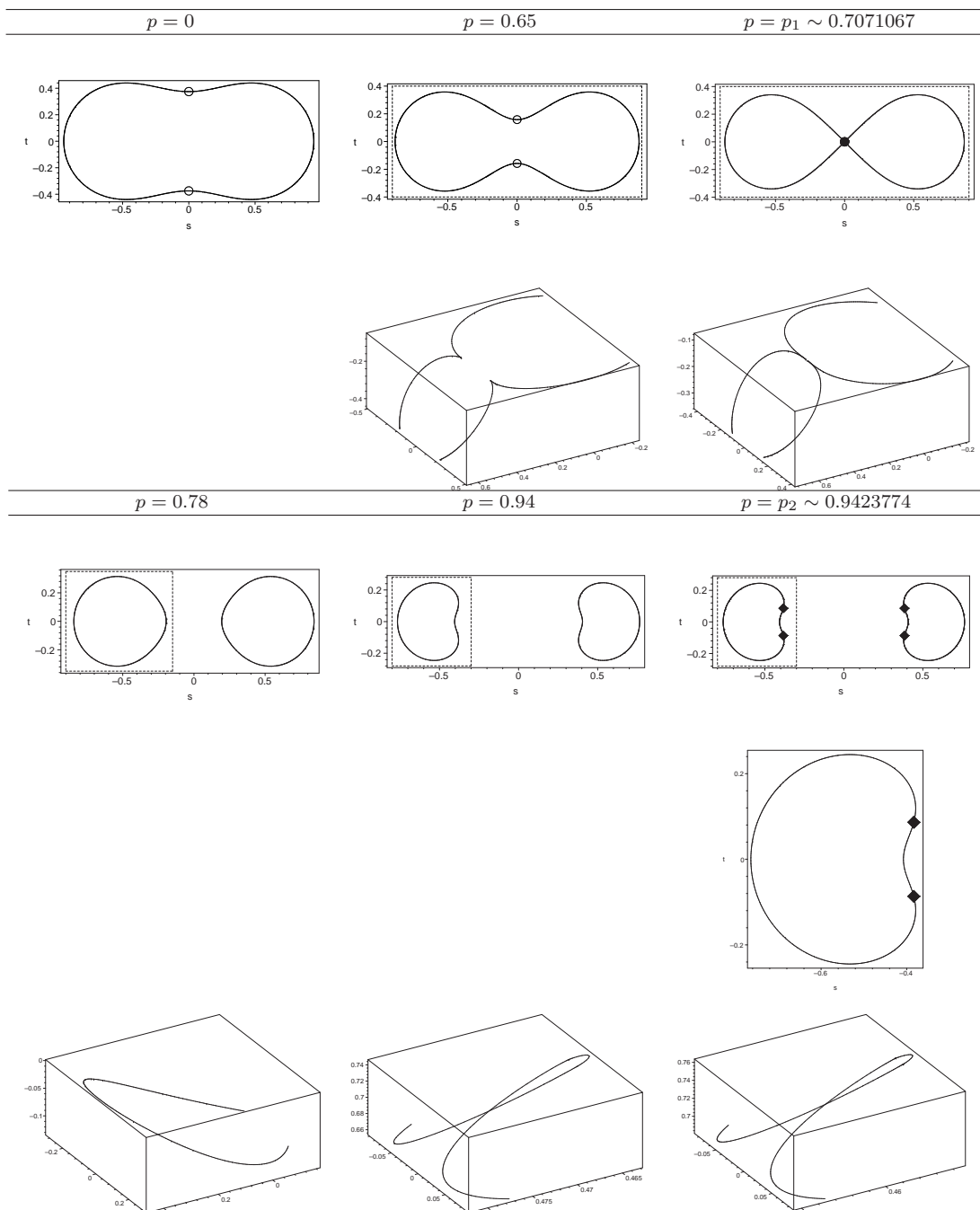


FIGURE 3. The curve  $C$  and the curve  $\mathcal{C}$  (1)

REFERENCES

- [Arnold 1976] V. I. ARNOL'D, *Wave front evolution and equivariant Morse lemma*, Comm. pure appl. Math., **29**(1976), 557–582.
- [Gálvez et al. 2000] J. A. GÁLVEZ, A. MARTÍNEZ AND F. MILÁN, *Flat surfaces in hyperbolic 3-space*, Math. Annalen, **316** (2000), 419–435.
- [Iwasaki et al. 1991] K. IWASAKI, H. KIMURA, S. SHIMOMURA AND M. YOSHIDA, *FROM GAUSS TO PAINLEVÉ – A MODERN THEORY OF SPECIAL FUNCTIONS*, Vieweg Verlag, Wiesbaden, 1991.

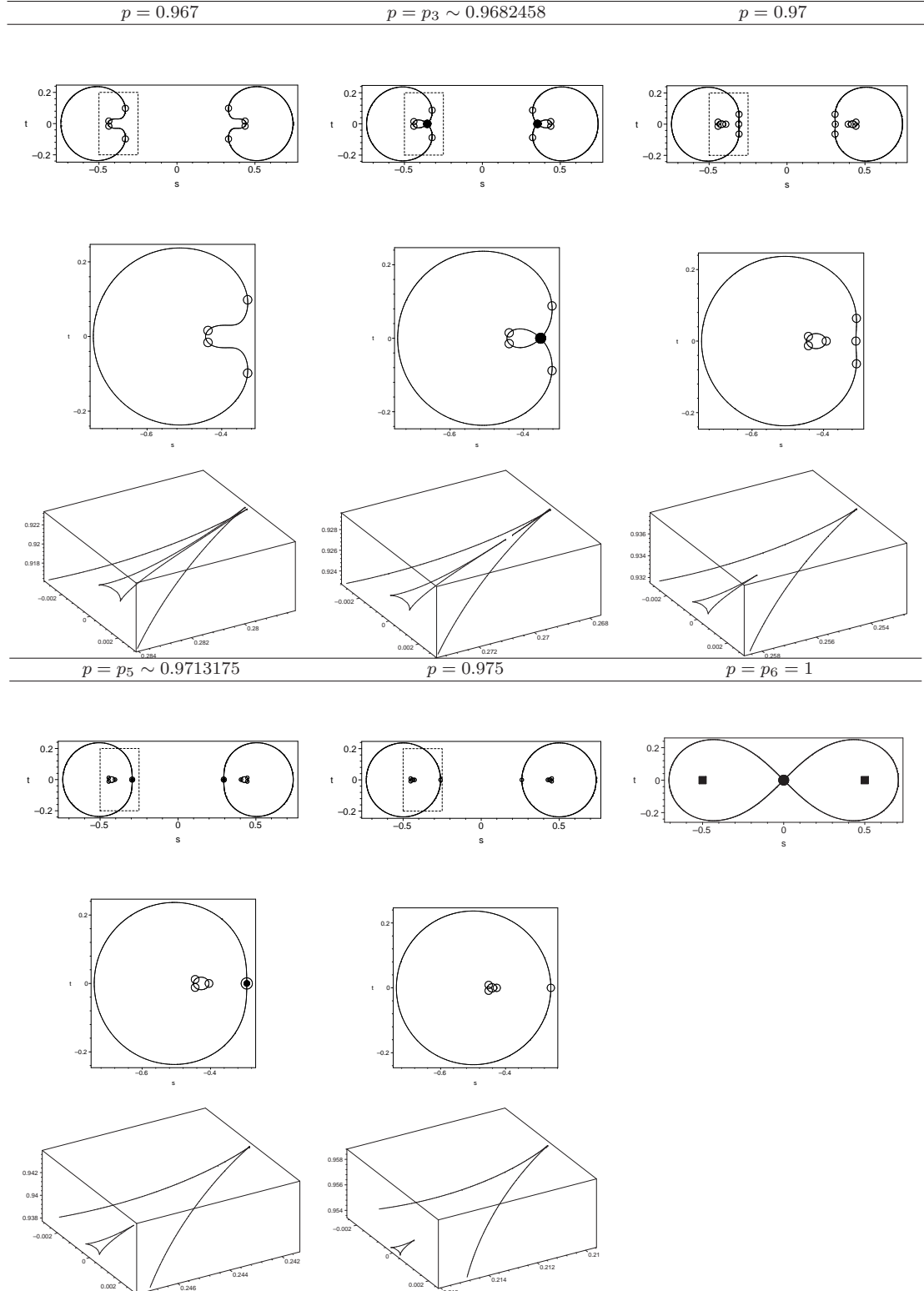


FIGURE 4. The curve  $C$  and the curve  $\mathcal{C}$  (2)

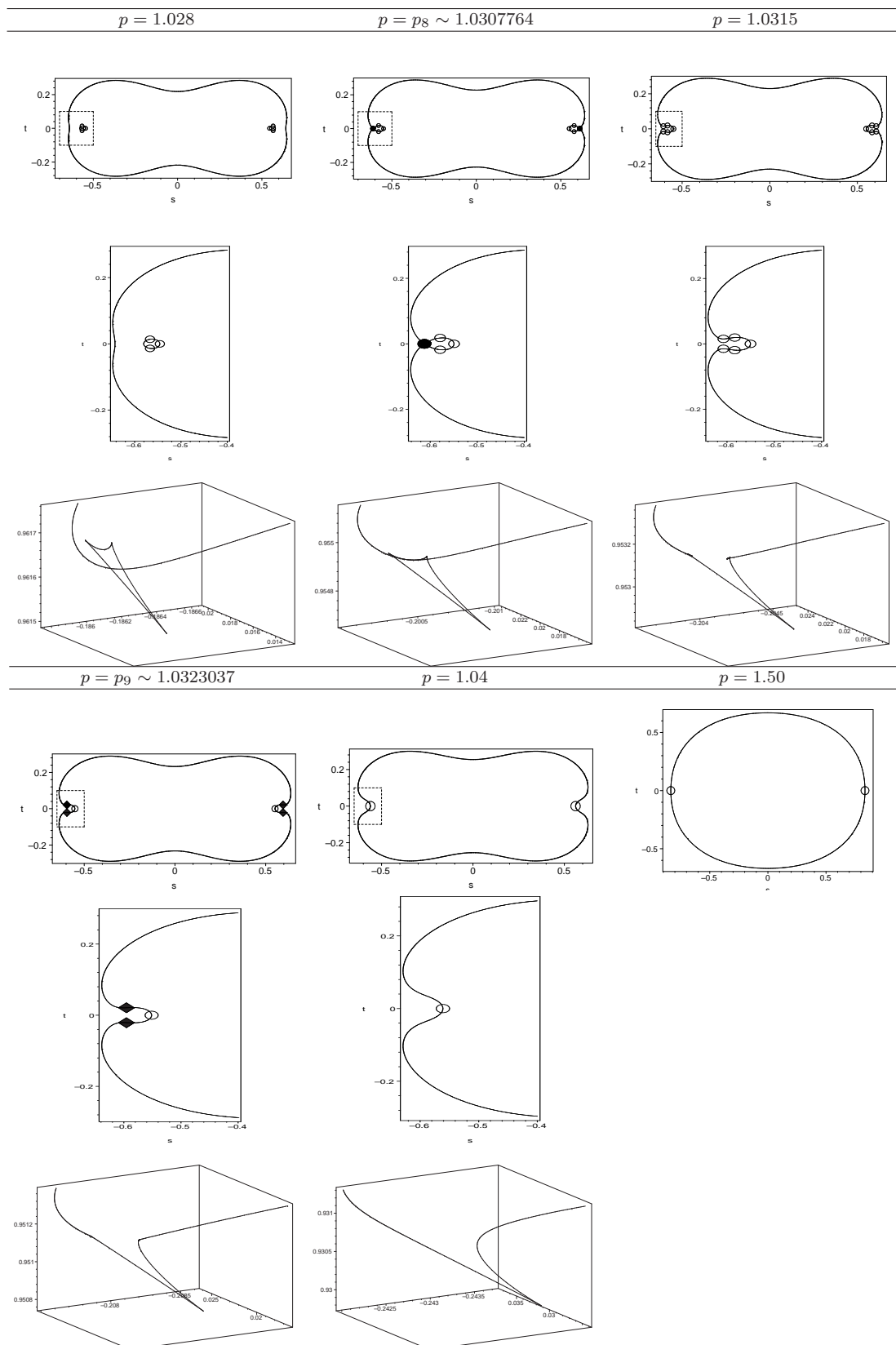


FIGURE 5. The curve  $C$  and the curve  $\mathcal{C}$  (3)

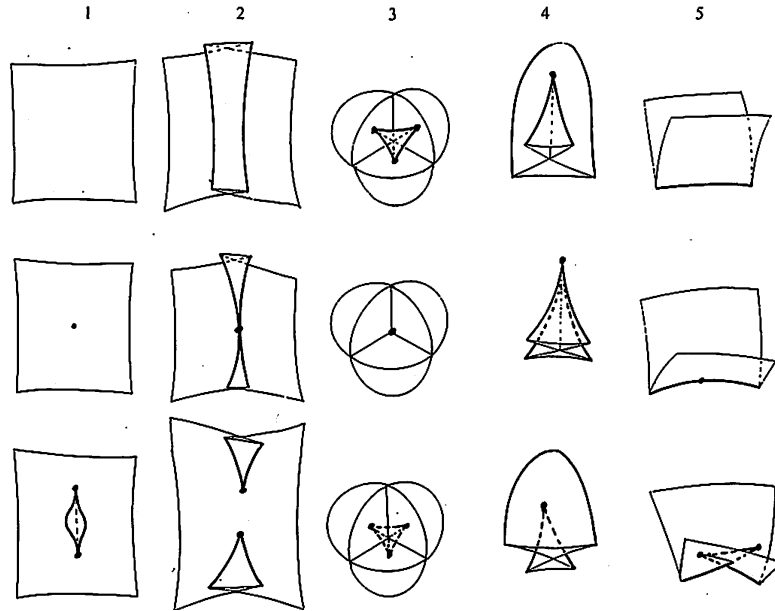


FIGURE 6. Confluence of swallowtail singularities from [Langevin et al. 1995], p. 547

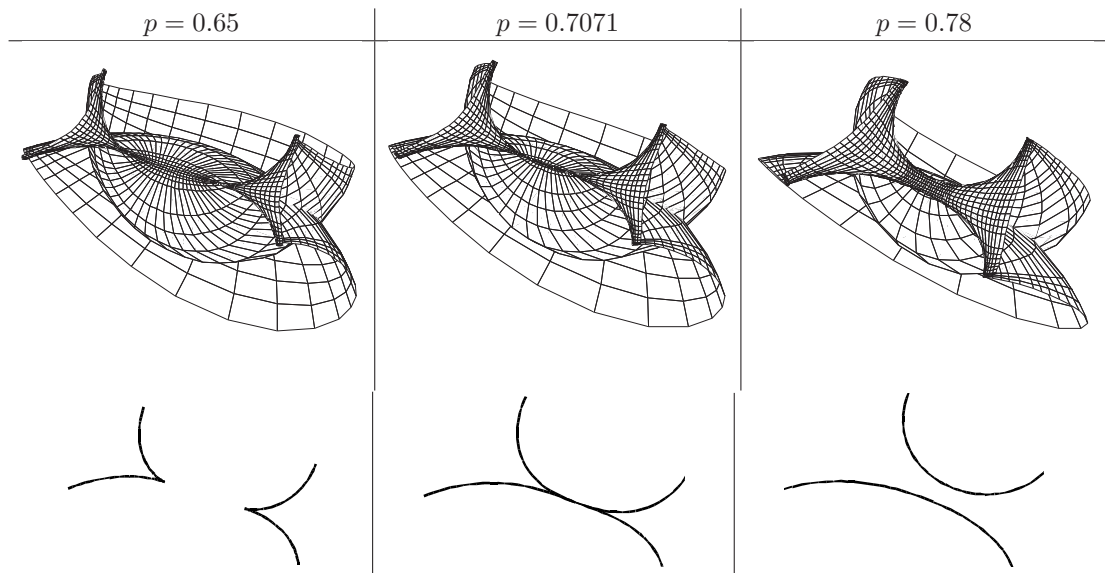
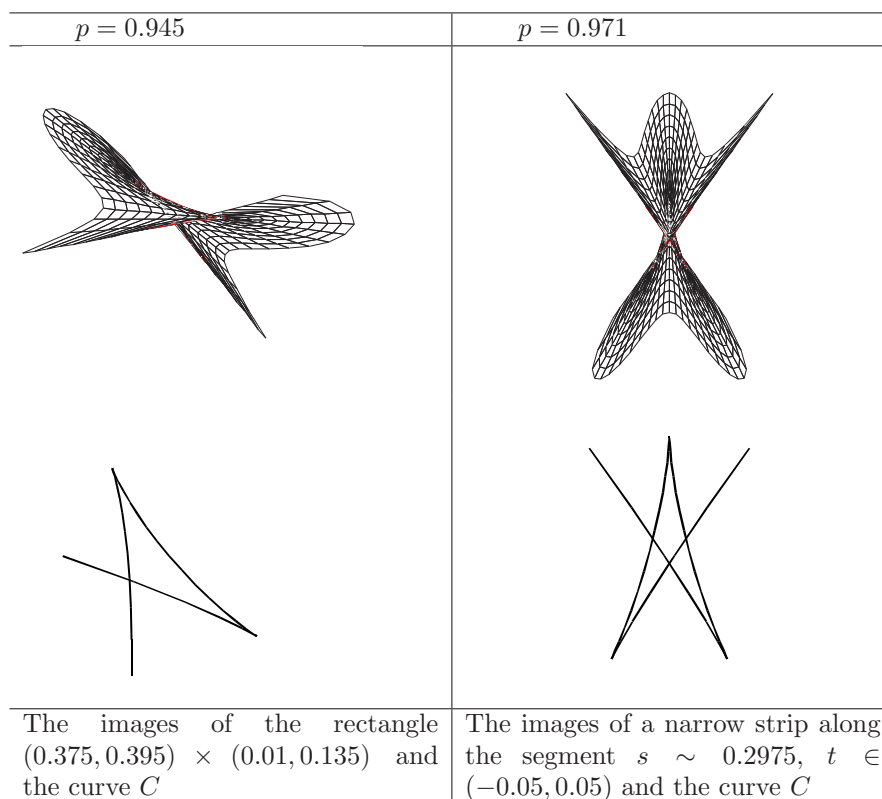


FIGURE 7. The images under  $HS$  (1): the images of the square  $(-0.5, 0.5) \times (-0.5, 0.5)$  and the curve  $\mathcal{C}$  in it

[Jacobson 1975] N. JACOBSON, *Lectures in abstract algebra 3 : Theory of fields and Galois theory*, Graduate Texts in Math. 32, 1975, Springer.

FIGURE 8. The images under  $HS$  (2)

- [Kokubu et al. 2003] M. KOKUBU, M. UMEHARA AND K. YAMADA, *An elementary proof of Small's formula for null curves in  $PSL(2, \mathbf{C})$  and an analogue for Legendreian curves in  $PSL(2, \mathbf{C})$* , Osaka J. Math. **40**(2003), 697–715.
- [Kokubu et al. 2005] M. KOKUBU, W. ROSSMAN, K. SAJI, M. UMEHARA AND K. YAMADA, *Singularities of flat fronts in hyperbolic space*, Pacific J. Math. **221**(2005), 303–351.
- [Langevin et al. 1995] R. LANGEVIN, G. LEVITT AND H. ROSENBERG, *Classes d'homotopie de surfaces avec rebroussements et queues d'aronde dans  $\mathbf{R}^3$* , Can. J. Math. **47**(1995), 544–572.
- [Sasaki et al. 2006] T. SASAKI K. YAMADA AND M. YOSHIDA, *Hyperbolic Schwarz map for the hypergeometric equation*, preprint, math.CA/0609196; revised 2007.
- [Sasaki et al. 2007] T. SASAKI K. YAMADA AND M. YOSHIDA, *Derived Schwarz map of the hypergeometric differential equation and a parallel family of flat fronts*, preprint, 2007.
- [Yoshida 1997] M. YOSHIDA, *Hypergeometric Functions, My Love*, Vieweg Verlag, Wiesbaden, 1997.

(Noro) DEPARTMENT OF MATHEMATICS, KOBE UNIVERSITY, KOBE 657-8501, JAPAN  
*E-mail address:* [noro@math.kobe-u.ac.jp](mailto:noro@math.kobe-u.ac.jp)

(Sasaki) DEPARTMENT OF MATHEMATICS, KOBE UNIVERSITY, KOBE 657-8501, JAPAN  
*E-mail address:* [sasaki@math.kobe-u.ac.jp](mailto:sasaki@math.kobe-u.ac.jp)

(Yamada) FACULTY OF MATHEMATICS, KYUSHU UNIVERSITY, FUKUOKA 812-8581, JAPAN  
*E-mail address:* [kotaro@math.kyushu-u.ac.jp](mailto:kotaro@math.kyushu-u.ac.jp)

(Yoshida) FACULTY OF MATHEMATICS, KYUSHU UNIVERSITY, FUKUOKA 810-8560, JAPAN  
*E-mail address:* [myoshida@math.kyushu-u.ac.jp](mailto:myoshida@math.kyushu-u.ac.jp)

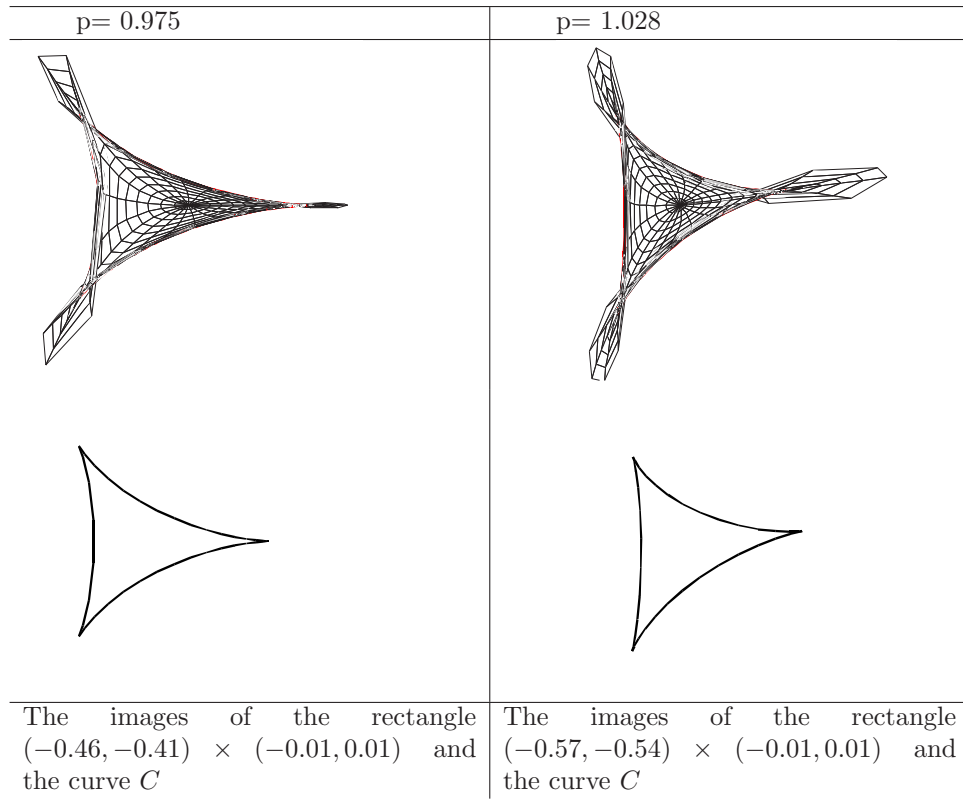


FIGURE 9. The images under  $HS$  (3)